# siRNA-mediated gene knockdown via electroporation in hydrozoan jellyfish embryos

[1] Tokiha Masuda-Ozawa, [2] Sosuke Fujita, [3] Ryotaro Nakamura, [3] Hiroshi Watanabe, [2] Erina Kuranaga, and [1,4] Yu-ichiro Nakajima*

1. Frontier Research Institute for Interdisciplinary Sciences, Tohoku University, Sendai, Japan
2. Graduate School of Life Sciences, Tohoku University, Sendai, Japan
3. Evolutionary Neurobiology Unit, Okinawa Institute of Science and Technology Graduate University, Okinawa, Japan
4. Graduate School of Pharmaceutical Sciences, The University of Tokyo

*Author for correspondence e-mail: nakaji97@g.ecc.u-tokyo.ac.jp
Tel: +81-3-5841-4863

**Running title**: **siRNA gene knockdown in jellyfish embryos**
**Main text**: 6487 words (Abstract: 258 words)
**Figures**: 5 **Supplementary information** (Figures: 7; Table: 5)
**Keywords**: siRNA, electroporation, cnidarian, hydrozoan, jellyfish, *Clytia, Cladonema*

## Abstract

As the sister group to bilaterians, cnidarians stand in a unique phylogenetic position that provides insight into evolutionary aspects of animal development, physiology, and behavior. While cnidarians are classified into two types, sessile polyps and free-swimming medusae, most studies at the cellular and molecular levels have been conducted on representative polyp-type cnidarians and have focused on establishing techniques of genetic manipulation. Recently, gene knockdown by delivery of short hairpin RNAs into eggs via electroporation has been introduced in two polyp-type cnidarians, *Nematostella vectensis* and *Hydractinia symbiolongicarpus*, enabling systematic loss-of-function experiments. By contrast, current methods of genetic manipulation for most medusa-type cnidarians, or jellyfish, are quite limited, except for *Clytia hemisphaerica*, and reliable techniques are required to interrogate function of specific genes in different jellyfish species. Here, we present a method to knock down target genes by delivering small interfering RNA (siRNA) into fertilized eggs via electroporation, using the hydrozoan jellyfish, *Clytia hemisphaerica* and *Cladonema paciificum*. We show that siRNAs targeting endogenous *GFP1* and *Wnt3* in *Clytia* efficiently knock down gene expression and result in known planula phenotypes: loss of green fluorescence and defects in axial patterning, respectively. We also successfully knock down endogenous *Wnt3* in *Cladonema* by siRNA electroporation, which circumvents the technical difficulty of microinjecting small eggs. *Wnt3* knockdown in *Cladonema* causes gene expression changes in axial markers, suggesting a conserved Wnt/β-catenin-mediated pathway that controls axial polarity during embryogenesis. Our gene-targeting siRNA electroporation method is applicable to other animals, including and beyond jellyfish species, and will facilitate the investigation and understanding of myriad aspects of animal development.

## Introduction

The phylum Cnidaria is the sister group to Bilateria, having separated from their common ancestor over 500 million years ago. Cnidarians have diversified their morphologies across an array forms, including corals, sea anemones, hydroids, and jellyfish, all of which are divided into two clades: Anthozoa and Medusozoa. The two differ in that Anthozoa includes only sessile polyp-type animals, while Medusozoa (Hydrozoa, Staurozoa, Scyphozoa, and Cubozoa) contains two forms: polyp and medusa, commonly known as jellyfish (Fig. 1A)[1,2]. The life cycle of most, though not all, jellyfish consists of five forms: gametes, fertilized eggs, planulae, polyps, and medusae[3]. Fertilized eggs undergo embryogenesis to become planula larvae, which metamorphose into sessile polyps. While vegetatively-growing polyps give rise to free-swimming medusae through the process of budding or strobilization, medusae sexually reproduce by releasing gametes. Due to their unique phylogenetic position, studies using cnidarians have provided evolutionary insight into development, regeneration, and behaviors in multicellular animals[1,4,5]. Despite divergent morphologies and lifestyles among cnidarians, to date, the molecular and cellular understanding of cnidarians has been acquired primarily using polyp-type animals such as the anthozoan *Nematostella vectensis* and the hydrozoan *Hydra* and *Hydractinia*. By contrast, jellyfish biology remains largely unestablished.

Among jellyfish species, the hydrozoan *Clytia hemisphaerica* is the best-studied laboratory model[6,7]. The well-established methodology for maintaining and propagating animals ensures a reliable source for daily experiments[8]. Transparent and small-sized medusae make whole-mount visualization achievable, and relatively large-sized eggs (~180 μm diameter) enable different manipulations via microinjection (Fig. 1B). Indeed, gene silencing by morpholino oligos and mRNA microinjection as well as gene knockout via CRISPR/Cas9 allow for the investigation of functions of genes of interest[9-13]. Furthermore, the *Clytia* genome assembly is complete, and transcriptome profiles are available for various stages and tissues, even at the single-cell level, which creates the foundation for research at the molecular level[12,14-18]. These resources and techniques, together with recently-established transgenesis[19], have accelerated research into numerous facets of distinct *Clytia* life stages. While initial studies focused on

95 embryogenesis, current research topics using *Clytia* include gametogenesis,
96 regeneration, and behavior exhibited by adult medusa [9,10,12,17,19,20].
97 Compared to the established model jellyfish *Clytia*, the hydrozoan *Cladonema*
98 *pacificum* is an emerging model that has recently been utilized for various studies in
99 development, regeneration, and physiology[21]. The ease of rearing all stages of
100 *Cladonema* without a filtration system or large water tank, along with their high
101 spawning rate, enable easy lab maintenance. Small-sized medusae with branched
102 tentacles allow for investigations of body size control and tentacle morphogenesis (Fig.
103 1C)[22-24]. *Cladonema* gametogenesis is regulated by a light-dark cycle as in *Clytia*, and
104 recent work has identified the neuropeptides involved in oocyte maturation[25].
105 Furthermore, *Cladonema* medusae possess eyes with a complex structure that includes
106 lenses (ocelli) in their tentacle bulbs, and studies using the closely related species
107 *Cladonema radiatum* have identified conserved light-sensitive opsins and regulators of
108 eye formation (*Pax*, *Six*, and *Eya*)[25-29], providing a model for the evolutionary
109 developmental biology of photoreceptor organs. Despite these attractive features of
110 *Cladonema* as a laboratory animal, no genome assembly or transcriptome is currently
111 available, and genetic manipulation techniques are only just being developed. One
112 major technical issue in manipulating *Cladonema* is their small eggs—with a diameter of
113 approximately 60 μm (Fig. 1C), regular microinjection is quite difficult. Establishing
114 genetic manipulations is required to facilitate the in-depth investigations needed to
115 further understand the biology of *Cladonema*, and an alternative method that eliminates
116 the need for microinjection would greatly facilitate that objective.
117 RNA interference (RNAi), the phenomenon of double stranded RNA (dsRNA)
118 mediated silencing of target genes, has been widely exploited in living organisms to
119 analyze gene function[30], primarily using chemically- or *in vitro*-synthesized double-
120 stranded small interfering RNAs (siRNAs) or vector-based short hairpin RNAs
121 (shRNAs)[31]. In cnidarians, siRNA-mediated gene silencing was initially applied to
122 *Nematostella* and *Hydra* polyps via soaking or electroporation[32-34]. More recently, gene
123 knockdown via shRNA microinjection or electroporation into eggs has been utilized in
124 studies with *Nematostella* and *Hydractinia* to show efficient reduction in gene
125 expression and associated phenotypes in early developmental stages[35-38]. In particular,
126 shRNA delivery via electroporation, which does not require the rigors of microinjection,

127 allows for the experimental gene knockdown of large numbers of individuals
128 simultaneously[36,38], opening up the possibility of manipulating genes in different aquatic
129 animals, even those that produce very small eggs like *Cladonema*.
130 The mechanism of RNAi-mediated gene repression after introducing foreign
131 dsRNA into cells involves the microRNA (miRNA) pathway, an endogenous gene
132 repression machinery conserved in both animals and plants[39]. In cnidarians, the
133 presence of the miRNA pathway has been demonstrated in *Nematostella* and
134 *Hydra*[32,40,41]. However, little is known about the endogenous RNAi pathway, especially
135 the presence and roles of miRNAs and the miRNA-related genes, in jellyfish such as
136 *Clytia* and *Cladonema*. Furthermore, in mammalian cultured cells, siRNAs can induce
137 gene repression independent of endogenous dsRNA processing factors, while shRNAs
138 cannot[42,43]. On this basis, we selected siRNA instead of shRNA for gene knockdown to
139 avoid the potential pitfall of dsRNA processing in jellyfish.
140 Here we report a gene knockdown method for jellyfish embryos with siRNA via
141 electroporation. Using two hydrozoan species, *Clytia hemisphaerica* and *Cladonema*
142 *pacificum*, we demonstrate that siRNA delivery into fertilized eggs effectively reduces
143 the expression of endogenous genes. We also confirm the known loss-of-function
144 phenotypes in *Clytia* after knocking down *GFP1* or *Wnt3*, which are induced in a dose-
145 dependent manner with siRNA. We further show that knockdown of *Wnt3* in *Cladonema*
146 embryos results in the reduction of gene expression of the oral marker *Brachyury* in
147 planula, implicating the Wnt/β-catenin pathway in the control of oral-aboral patterning.
148 Overall, our siRNA-mediated knockdown approach allows for the manipulation of a
149 large number of embryos through electroporation and enables functional analysis of
150 early development, providing a new experimental platform applicable to different jellyfish
151 species and other marine invertebrates.
152
153
154 ## Materials and Methods
155
156 ### Animal culture and spawning induction
157 *Clytia hemisphaerica* (Z11, Z4B as females and Z4C2, Z23 as males) and *Cladonema*
158 *pacificum* (6W as females and UN2 as males) were used for this research.

159 *Clytia hemisphaerica* were cultured using a previously reported method[8] with a
160 few modifications. Artificial sea water (ASW) was prepared using 220 g SEA LIFE
161 (Marin Tech) per 5L MilliQ water (Merk Millipore) with antibiotics (40 units/ml of penicillin
162 and 40 µg/ml of streptomycin). Medusae, embryos, and planula larvae were maintained
163 at 20ºC. Medusae were fed daily with Vietnamese brine shrimp (A&A Marine LLC, Elk
164 Rapids, MI, USA). Spawning timing was controlled by a 13 hours (h) dark /11 h light
165 cycle, and spawning was induced by light. Male and female medusae were transferred
166 into V-7 cups (AS ONE) before spawning (60 min for male and 90 min for female after
167 light stimulation).
168 *Cladonema pacificum* were cultured as previously described[23]. *Cladonema*
169 medusae were maintained at 22ºC in ASW, which was prepared using SEA LIFE (Marin
170 Tech) dissolved in tap water with chlorine neutralizer (Coroline off, GEX Co. ltd) (24
171 p.p.t) and antibiotics (40 units/ml penicillin and 40 µg/ml of streptomycin). Spawning
172 timing was controlled by a 30 min dark/23.5 h light cycle, and spawning of male and
173 female gametes was induced by dark stimulation. Before dark stimulation, adult females
174 and males were separately transferred into V7 cups (AS ONE) and 60 mm dishes (BD),
175 respectively.
176 *Nematostella vectensis* were cultured as previously described[44], with a few
177 modifications. Briefly, adult animals were maintained in brackish water at a salinity one-
178 third of artificial seawater (35 g/l, pH 7.5-8.0, SEA LIFE, Marin Tech) and fed with
179 freshly hatched artemia twice per week. Spawning induction was performed at 26°C
180 under light for at least 11 h.
181
182
183 **siRNA and shRNA**
184 siRNA sequences (19 mer RNA + 2 mer DNA) for *CheGFP1*, *CheWnt3*, and *CpWnt3*
185 were designed based on their CDS sequences by Nippon Gene Co., Ltd, and siRNA
186 duplexes were synthesized by manufacturers (Nippon Gene Co., Ltd and Sigma-
187 Aldrich, Merk). Lyophilized siRNA was resuspended in RNase free water to a final
188 concentration of 6 µg/µl as stock solution. The siRNA stock solution was diluted with
189 RNase free water to a total volume of 10 µl and then added to 90 µl of fertilized eggs in
190 15% Ficoll ASW just prior to electroporation.

191 shRNAs were synthesized as described in previous reports[36,38]. Briefly, shRNAs
192 were synthesized by *in vitro* transcription (IVT) from double stranded DNA templates
193 using the AmpliScribeTM T7-flashTM transcription kit (Lucigen, Inc.) and were purified
194 using Direct-Zol TM RNA Miniprep kits (Zymo Research, R2070). Concentrations of
195 shRNA was measured with a NanoDrop One (Thermo fisher).
196
197
198 **Collection of gametes and electroporation for *Clytia* and *Cladonema* fertilized**
199 **eggs**
200 For the preparation of gametes, sexually-mature *Clytia* medusae were treated following
201 a previously reported method[8], partially modified to fit our experimental equipment.
202 Adult medusae were maintained on a 13 h dark/11 h light cycle, and light stimuli
203 induced gametogenesis in 60 min for sperms and 90 min for eggs (Fig. 2A). For
204 *Cladonema pacificum*, sexually-mature medusae were maintained on a 30 min
205 dark/23.5 h light cycle. Dark stimulation induced gametogenesis in 25 min. Unfertilized
206 eggs were collected and resuspended in 15% Ficoll (Nacalai tesque, Japan) in ASW to
207 prevent the eggs settling from at the bottom of the microtube or sticking to the microtube
208 surface, keeping the egg solution homogeneous (Fig. 2B)[36,38].
209 Unfertilized *Clytia* and *Cladonema* eggs were collected in dishes and transferred
210 into 1.5 ml tubes coated with Ficoll (Nacalai tesque, Japan) to prevent the eggs from
211 sticking to the tubes. Sperm water was added into eggs, and the eggs and sperm were
212 incubated for 5 min at room temperature (20-22ºC). The sperm water was then
213 removed, and fertilized eggs were resuspended in 15% Ficoll in ASW, at which point
214 siRNA or shRNA was added into fertilized egg solution. The fertilized egg and RNA
215 mixture was carefully transferred into a 4 mm cuvette and placed into the shockpod
216 cuvette chamber connected to the Gene Pulser Xcell (Bio-Rad). In most experiments,
217 the Gene Pulser Xcell was used for pulsing with a square wave voltage of 50 V and a
218 single pulse duration of 25 ms, except when optimizing electroporation conditions
219 (Supplementary Figs 1-2). After electroporation, fertilized eggs were transferred to a
220 dish, and incubated for 10 min. The 15% Ficoll solution was removed and replaced with
221 new ASW, and the samples were incubated at 20-22ºC.
222

223

224 **Collection of egg sacs, dejellying, and electroporation of *Nematostella* fertilized**
225 **eggs**

226 The collection of egg sacs, dejellying, and electroporation steps were performed as
227 previously described[36] with several modifications. Briefly, unfertilized egg sacs were
228 incubated in culture media with sperm at 20-25ºC for 30 min. The fertilized egg sacs
229 were then dejellied in freshly prepared L-Cysteine solution (0.04 g/ml, Nacalai tesque, in
230 brackish water; pH adjusted by 5N NaOH at 7.5-8.0) on a shaker for 10 min. The
231 dejellied eggs were rinsed with brackish water before they were suspended in Ficoll
232 solution (Sigma-Aldrich, in brackish water) at a final concentration of 15%. The
233 suspended eggs and siRNA (5 µg/µl stock solution, in MilliQ) were transferred to a 4
234 mm cuvette (Bio-Rad) with a final volume of 200 µl and were gently mixed. The Bio-Rad
235 Gene Pulser Xcell was used for pulsing, with a square wave voltage of 50 V and a pulse
236 duration of 25 ms. The samples were transferred to a 100 mm dish and maintained in
237 brackish water for 3 days.

238

239

240 **Imaging**

241 GFP and Rhodamine fluorescent imaging as well as bright field imaging, including *in*
242 *situ* hybridization imaging, were taken with an Axio Zoom V16 (ZEISS), and image
243 processing was done with ZEN 3.4 blue edition (ZEISS) and Fiji/ImageJ software[45].
244 Intensity of mean values of green fluorescence was measured using the average
245 brightness (pixel value) of the pixels. To prevent planula movement, we added 0.5 M
246 sodium azide (final concentration was less than 0.25M).

247

248

249 **Morphological quantification of planula larvae**

250 After *Wnt3* knockdown by siRNA electroporation of *Clytia* or *Cladonema*, we
251 approximated the planula body shape into a two dimensional ellipse, measured both the
252 long and short axes (Figs. 4C and 5D), and calculated the aspect ratio of those values
253 using Fiji/ImageJ software (Figs, 4D, 5E).

254

255

256 **RT-qPCR**

257 For *Clytia* and *Cladonema* samples, total RNA was extracted with RNeasy Mini or Micro
258 kits (Qiagen). Lysate was treated with DNaseI (Qiagen) for 15 min at room temperature
259 (RT). cDNA was synthesized with the PrimeScript II 1st strand synthesis kit (Takara bio).
260 RT-qPCR was performed with CFX connect (Bio-Rad) using iTaqTM universal SYBER
261 Green Supermix (Bio-Rad) or the QuantStudio 6 Flex Real-Time PCR System (Thermo
262 Fisher) using TB Green Premix Ex TaqII (Tli RNaseH Plus) (Takara, RR820). Gene
263 expression was normalized to the housekeeping gene, *EF1alpha* or *F-actin capping*
264 *protein subunit beta*, and the delta-delta-ct method was used for quantification (CFX
265 maestro software, Bio-Rad or QuantStudio 6 Flex Real-Time PCR System software,
266 Thermo Fisher).

267 For *Nematostella* samples, total RNA was extracted using the RNeasy Mini Kit
268 and RNase-Free DNase Set (Qiagen). cDNA synthesis was conducted using the
269 SuperScript IV First-Strand Synthesis System (Thermo Fisher). RT-qPCR was
270 performed with the StepOnePlusTM Real-Time PCR System (Applied Biosystems,
271 Thermo Fisher) using PowerUP SYBR Green Master Mix (Thermo Fisher). Gene
272 expression was normalized to the housekeeping gene, *NvEf1alpha,* and the delta-delta-
273 ct method was used for quantification (StepOne™ and StepOnePlus™ Software v2.3).

274

275

276 ***In situ* hybridization**

277 Purified total RNA was reverse transcribed into cDNA by PrimeScript™ 2 1st strand
278 cDNA Synthesis Kit (TaKaRa). The target gene fragments (*Brachyury*, *CpBra*) were
279 amplified from a cDNA library. The primer sets used for PCR cloning are as follows:
280 *CpBra*: 5'-GCTCCCATAAGATCCGGTCG -3'(forward) and 5'-
281 TTTGTCGCAGTCGAAGACCA-3'(reverse), or 5'-GAACGGTGATGGACAGGTCA-
282 3'(forward) and 5'-GGATTCCAAGGATTGGGCGT-3'(reverse). PCR products were sub-
283 cloned into the TAK101 vector (TOYOBO). The resulting plasmids were used for RNA
284 probe synthesis with digoxigenin (DIG) labeling mix (Roche) and T7 or T3 RNA
285 polymerase (Roche), according to the insert direction.

286 Planula larvae were anesthetized in 50% 0.5 M $NaN_3$ in ASW for 5 min and fixed
287 overnight at 4°C with 4% paraformaldehyde (PFA) in ASW. Fixed samples were washed
288 three times with PBS containing 0.1% Tween-20 (PBST), followed by pre-hybridization
289 in hybridization buffer (HB buffer: 5×SSC, 50% formamide, 0.1% Tween-20, 50 µg/ml
290 tRNA, 50 µg/ml heparin) at 55°C for 2 h. Samples were hybridized with HB Buffer
291 containing the probes (final probe concentration: 0.5-1 ng/µL in HB Buffer) at 55°C
292 overnight and washed. The samples were incubated with 0.05% alkaline phosphatase
293 (AP)-conjugated anti-DIG antibodies (Roche) in 1% blocking reagent (Roche) in Maleic
294 acid buffer for 4 h at room temperature. Colorimetric reactions were performed by
295 NBT/BCIP (Roche) in alkaline phosphatase buffer (100 mM NaCl, 100 mM Tris-HCl (pH
296 9.5), 50 mM $MgCl_2$, 0.1% Tween-20) until the signals were detected.
297
298
299 **Sequence alignment and phylogenetic analysis**
300 Amino acid sequence alignment of Wnt3 and Wnt family proteins were performed by
301 ClustalW[46]. GenBank accession numbers and protein names are listed in
302 Supplementary Table 3 and 4. The alignment data was visualized on Jalview software[47].
303 Maximum likelihood (ML) tree calculation was inferred on ClustalW with the PhyML
304 bootstrap method. Branch supports were computed out of 100 bootstrapped trees. The
305 tree visualization was created using MEGA-X software[48].
306
307
308 **qPCR primers**

| Name | Sequence (5'->3') | |
|---|---|---|
| CpWnt3 qP FW | CAAATGTGGTCGATCAAACG | This study |
| CpWnt3 qP RV | TACGCCTTCTGCAACACTTG | This study |
| CpEF1-a_qPCR_F7 | GGTCAATCTCGTTCCCTCCA | This study |
| CpEF1-a_qPCR_R7 | TTTCCACCAGAGGTATCGGC | This study |
| CpBrachyury F | AAGGCGTATGTTTCCGGTCC | This study |
| CpBrachyury R | CAACGATGGTCTTCGACTGC | This study |
| CpFoxQ2a F | AGTTGGAGAAACAGCGTTCG | This study |
| CpFoxQ2a R | CCGTTCGCAAAGTCGTCAAA | This study |
| CpCapZbeta_qPCR_F | AAAGAAAGCTGGAGACGGTTCA | This study |
| CpCapZbeta_qPCR_R | GTAGTGGGCATTTCTTCCGC | This study |
| CheGFP1 qP F | TTGCTGTCCGAATAGTGCAG | Fourrage et al., 2014 Open Biol |

| | | |
|---|---|---|
| CheGFP1 qP RV | GACAACTCCTCCTCCGAGTG | Fourrage et al., 2014 Open Biol |
| CheGFP1_2 qP F | ACAATCGCGTCACACTTAAAGG | This study |
| CheGFP1_2 qP RV | CGTTGTTTTCTTTGTCCGGC | This study |
| CheWnt3 qP F | ATCATGGCAGGTGGAAACTC | Leclère et al., 2012 Dev Biol |
| CheWnt3 qP RV | CCCCATTTCCAACCTTCTTC | Leclère et al., 2012 Dev Biol |
| CheEF1a qP F | TGCTGTTGTCCCAATCTCTG | Leclère et al., 2012 Dev Biol / Fourrage et al., 2014 Open biol |
| CheEF1a qP RV | AAGACGGAGTGGTTTGGATG | Leclère et al., 2012 Dev Biol / Fourrage et al., 2014 Open biol |
| NvEf1alpha FW | GGTTGCCTCTTCGCTTACCACT | This strudy |
| NvEf1alpha RV | CGTTCCTGGCTTTAGGACAC | This study |
| NvBra1_Fw_1032 | CGGGCTCACACTCTCACTTA | This study |
| NvBra1_Rv1174 | CTTGCGGTATGGTGTTCCAG | This study |
| | | |

## siRNA design

| Name | Sequence (5'->3') | | ORF |
|---|---|---|---|
| siCheGFP1_1 sense | CCAUCAGCUUCGAAAAUGAdTdT | This study | HQ397706.1 |
| antisense | UCAUUUUCGAAGCUGAUGGdTdT | This study | |
| siCheGFP1_2 sense | UGAUGGCGCUUAUAAAGUUdTdT | This study | HQ397706.1 |
| antisense | AACUUUAUAAGCGCCAUCAdTdT | This study | |
| siCheGFP1_3 sense | CGGACUCAUUCUUCAAAAAdTdT | This study | HQ397706.1 |
| antisense | UUUUUGAAGAAUGAGUCCGdTdT | This study | |
| siCheWnt3_1 sense | GCAUGUGACUGUAAAUUUAdTdT | This study | EU374721.1 |
| antisense | UAAAUUUACAGUCACAUGCdTdT | This study | |
| siCheWnt3_2 sense | ACAGCUUGGUAAAAUGUUAdTdT | This study | EU374721.1 |
| antisense | UAACAUUUUACCAAGCUGUdTdT | This study | |
| siCpWnt3_1 sense | GUGGAACUGUAGUGUUUCAdTdT | This study | EU374721.1 |
| antisense | UGAAACACUACAGUUCCACdTdT | This study | |
| siCpWnt3_2 sense | AGCGUGUGCUGAAGGUAAAdTdT | This study | EU374721.1 |
| antisense | UUUACCUUCAGCACACGCUdTdT | This study | |
| siNvBra1_1 sense | GAAGAGAUCACGAGUCUAAdTdT | This study | AF540387.2 |
| antisense | UUAGACUCGUGAUCUCUUCdTdT | This study | |
| siNegative_Control-1 for Nv sense | GCAACACGCAGAGTCGTAAdT | Same sequence as Karabulut et al, 2019 Dev Biol | |
| antisense | TTACGACTCTGCGTGTTGCdT | Same sequence as Karabulut et al, 2019 Dev Biol | |

312

313 **shRNA template**

| Name | Sequence (5'->3') | |
|---|---|---|
| CheWnt3_SI1_F | TAATACGACTCACTATA GCATGTGACTGTAAATTTA TTCAAGAGA TAAATTTACAGTCACATGC TT | This study |
| CheWnt3_SI1_R | AAGCATGTGACTGTAAATTTATCTCTTGAATAAATTTAC AGTCACATGCTATAGTGAGTCGTATTA | This study |
| CheWnt3_SI2_F | TAATACGACTCACTATA ACAGCTTGGTAAAATGTTA TTCAAGAGA TAACATTTTACCAAGCTGT TT | This study |
| CheWnt3_SI2_R | AAACAGCTTGGTAAAATGTTATCTCTTGAATAACATTTT ACCAAGCTGTTATAGTGAGTCGTATTA | This study |

314

315

316 **Graphs and statistical analysis**

317 All graphs were prepared in Excel. To assess phenotypes and RT-qPCR statistical
318 significance, we used the percentage values and delta-delta-Ct values to perform two-
319 tailed Student's t tests, except in Figure 5F, where a one-tailed Student's t test was
320 used. For statistics related to fluorescence intensity mean value and aspect ratio,
321 Kolmogorov–Smirnov normality tests were used. All statistical tests were performed at
322 https://www.socscistatistics.com.

323

324

325 ## Results

326

327 **Optimization of electroporation conditions**

328 In both hydrozoan jellyfish *Clytia hemisphaerica* and *Cladonema pacificum*,
329 gametogenesis is regulated by light-dark transitions[6,49]. A previous report showed that
330 *Clytia* medusae release eggs within 110-120 min and sperm within 60-90 min upon light
331 illumination after 3-8 h of darkness[12]. *Cladonema pacificum*, which live along coastal
332 areas in Japan, exhibit two types of gametogenesis depending on habitat: the dark-light
333 transition (light stimulation type) and the light-dark transition (dark stimulation type),
334 respectively. Dark stimulation *Cladonema* medusae, which we used in this study,
335 release eggs or sperm within 30 min of dark stimulus after 20-24 h of constant exposure
336 to light[25,49]. By utilizing the characteristic gametogenesis of these jellyfish species, we
337 can control egg/sperm release to induce fertilization at any time of day. Indeed, we

338 routinely obtained *Clytia* sperm within 60 min and *Clytia* eggs within 90 min of light on a
339 13h dark/11h light cycle (Fig. 2A). Similarly, we collected gametes from *Cladonema*
340 within 25 min of dark stimulation on a 23.5h light/30 min dark cycle (Fig. 2A).
341 To determine optimal electroporation parameters, we first tested different
342 electroporation conditions and monitored the delivery efficiency of the red fluorescent
343 dye Rhodamine-Dextran into unfertilized *Clytia* and *Cladonema* eggs (Supplementary
344 Figs. 1-2). Given that the average molecular weight of siRNA (21-mer, ~13,300 Da) is
345 similar to the molecular size of Rhodamine-Dextran (10,000 Da), electroporation trials
346 with Rhodamine-Dextran can visually confirm that small molecules are incorporated into
347 jellyfish eggs, as previously shown in *Hydractinia* eggs[38]. The collected eggs were
348 suspended in 15% Ficoll artificial seawater to prevent precipitation and to make a
349 homogeneous solution (Fig. 2B)[36,38]. We performed electroporation trails for
350 Rhodamine-Dextran using a cuvette with a 4 mm gap and tested several conditions of
351 voltage (V) and pulse length time (milliseconds, ms) using a conventional
352 electroporation system (Fig. 2C). As previous work showed that increasing the number
353 of pulses does not increase the Dextran delivery rate but decreases the survival rate of
354 embryos[38], we fixed the number of pulses to one and incubated unfertilized eggs with 1
355 mg/ml Dextrane-Rhodamine solution. *Clytia* eggs have little autofluorescence in the red
356 channel, and without electroporation (No EP), red fluorescence was rarely detected in
357 unfertilized eggs (Fig. 2D and Supplementary Fig. 1A). We compared the eight different
358 electroporation conditions and found that the rhodamine fluorescence was detected in
359 *Clytia* eggs and correlated with the strength of electric voltage, as long as the voltage
360 was in the range of 50-100 V（Supplementary Figs. 1B-1D）. By contrast, when the
361 voltage exceeded 200 V, the eggs ruptured from physical damage, and cellular debris
362 was observed（Supplementary Figs, 1E-1G）.
363 We performed similar electroporation trials on unfertilized *Cladonema* eggs under
364 eight different conditions. While red autofluorescence was negligible in the *Cladonema*
365 eggs in the absence of electroporation (Fig. 2D and Supplementary Fig. 2A),
366 Rhodamine fluorescence was frequently detected with 50 V (Fig. 2D and
367 Supplementally Fig. 2E). In the more intense conditions beyond 100 V (Supplementally
368 Figs. 2F and 2G), the eggs were severely damaged. Based on these results, we
369 established the optimal electroporation conditions (50 V, 1 pulse, 25 ms) that provide

370 high frequency of Dextran-positive eggs and low levels of cell damage for both jellyfish
371 eggs (Fig. 2D). Of note, during the initial trials, we used unfertilized eggs, but we found
372 that the electroporation process severely affected the survival rate of subsequent
373 embryos. In the case of *Cladonema*, electroporation before fertilization severely
374 decreased the survival rate of fertilized eggs (7.04% at 1 h post fertilization) while
375 electroporation after fertilization did not influence the survival rate (No EP: 59.67%, With
376 EP: 60.15%) (Supplementary Table 1). This dissimilarity is likely due to the decrease of
377 fertilization rate after electroporation, and both elapsed time after spawning and physical
378 damage by electroporation can affect fertilization efficiency. Therefore, we decided to
379 conduct further electroporation experiments with fertilized eggs.
380
381
382 **Gene knockdown with siRNA in *Nematostella vectensis***
383 Before attempting gene knockdown via siRNAs electroporation in fertilized jellyfish
384 eggs, we first used *Nematostella vectensis,* where egg electroporation methodology has
385 been established[36]. We selected *Nematostella Brachyury* (*NvBra*), a gene expressed in
386 the blastopore margin that functions in the early embryo[50,51], as a target. After
387 electroporation of siRNA targeting *NvBra* in fertilized eggs, we examined *NvBra*
388 expression in planula larvae at 3 days-post-fertilization (dpf) by RT-qPCR and found
389 that *NvBra* expression was drastically suppressed compared to no electroporation
390 controls and negative control siRNAs (Supplementary Fig. 3). We further evaluated
391 survival rates after electroporation and confirmed that siRNA electroporation does not
392 severely affect survival rates of 3 dpf planula in any of the tested conditions
393 (Supplementary Table 2). These results suggest that siRNA delivery into fertilized eggs
394 via electroporation is an effective gene knockdown method that is comparable to the
395 effect of shRNA delivery into unfertilized eggs via electroporation[36], supporting our
396 attempt to perform gene knockdown via siRNA electroporation using fertilized jellyfish
397 eggs.
398
399
400 **Endogenous *GFP1* knockdown with siRNA in *Clytia hemisphaerica***

401 The hydrozoan jellyfish *Clytia* endogenously expresses green fluorescent proteins,
402 which are encoded by 14 genes grouped into 4 clusters (*CheGFP1-4*)[16]. The expression
403 pattern for each GFP changes by stage in the life cycle: for instance, *Clytia* eggs
404 express maternal *CheGFP2* mRNA, and planula larvae show typical ring-like *CheGFP1*
405 fluorescence in the lateral ectoderm at 3 dpf[11]. While *CheGFP1* gene expression
406 becomes dominant in the planula stage; *CheGFP2, CheGFP3,* and *CheGFP4* are
407 expressed in different tissues and organs in the medusa[52]. Momose *et al*. succeeded in
408 genome editing by injecting CRISPR/Cas9 targeting the endogenous *CheGFP1* into
409 fertilized eggs, and confirmed the knockout effect by loss of green fluorescence in 3 dpf
410 planula larvae[11]. In addition, *CheGFP1* is not essential for animal survival, which allows
411 for the monitoring of knockdown effects after embryogenesis. For these reasons, we
412 chose endogenous *CheGFP1* for the first target gene of siRNA knockdown.
413 In order to maximize the effect of gene knockdown, we used a combination of
414 three different siRNAs against *CheGFP1* (Accession No. HQ397706.1; Supplementary
415 Fig. 4A) in a mixture with a 1:1:1 ratio, and electroporated 600 ng/μl of siRNA mix (200
416 ng/μl per each siRNA) into fertilized eggs (Fig. 3A). To verify the effect of gene
417 knockdown, we measured green fluorescence intensity in 2 dpf planula and found that
418 siRNA (600ng/μl siRNA mix) electroporated embryos showed dramatically reduced
419 fluorescence intensity compared to the no-siRNA controls (Figs. 3B-D; mean intensity
420 value: $5.7\times10^3$ for 0 ng/μl control, $1.8\times10^3$ for 600 ng/μl). To evaluate the knockdown
421 effects at varying doses of siRNA, we next electroporated different concentrations of the
422 *CheGFP1* siRNA mix (0, 150, 300, and 600 ng/μl) into fertilized eggs. While control 3
423 dpf planulae with no-electroporation (No EP) as well as those with no-siRNA showed
424 typical ring-shape GFP fluorescence in the ectoderm, many planulae with *CheGFP1*
425 siRNA electroporation lost green fluorescence（Figs. 3E-3H）. To evaluate the GFP
426 knockdown effects, we classified planulae with typical GFP1 fluorescence as “wild type”
427 and planulae with reduced fluorescence as “reduced” for further quantification (Figs. 3I
428 and 3J). The percentage of wild type phenotype dramatically reduced in an siRNA dose-
429 dependent manner (Fig. 3K). To further quantify the above result on a molecular level,
430 we examined relative *CheGFP1* mRNA levels by RT-qPCR using the primer set that
431 was evaluated in a previously study[52]. Consistent with the image analysis results, we
432 confirmed a marked reduction of *CheGFP1* gene expression at different concentrations

433 of *CheGFP1* siRNA (Fig. 3L). These results demonstrate that siRNAs targeting
434 *CheGFP1* repress its expression upon electroporation and that the knockdown effects
435 are dose-dependent.
436 Given the presence of multiple *CheGFP1* loci (seven nearly identical *CheGFP1*
437 genes) in the *Clytia* genome[16], it was not clear whether three siRNAs against *GFP1*
438 sufficiently suppress gene expression in different versions of *CheGFP1*, particularly
439 those expressed in the planula stage (Supplementary Fig. 4A). We thus performed RT-
440 qPCR using the newly designed primer set that amplifies all seven *CheGFP1* genes and
441 found a dramatic reduction of gene expression upon electroporation of *CheGFP1*
442 siRNAs (600 ng/μl) (Supplementary Fig. 4B). Altogether, these results indicate that our
443 combination of *CheGFP1* siRNAs suppresses gene expression of *CheGFP1* in the
444 *Clytia* planula.
445
446
447 ***Wnt3* knockdown with siRNA in *Clytia hemisphaerica***
448 Since electroporation of siRNAs targeting endogenous *CheGFP1* was shown to be
449 effective, we next decided to investigate the effects of knocking down other genes that
450 play important roles in early development. Wnt3 is a secreted signaling protein in the
451 Wnt/β-catenin pathway that is involved in diverse developmental processes including
452 cell fate decisions and patterning[53,54]. In *Clytia*, *Wnt3* RNA is maternally localized to the
453 animal cortex, the future oral side of the embryo, and Wnt3 organizes axial patterning
454 as the main ligand for the Wnt/β-catenin pathway in the early embryonic stage[10]. After
455 embryogenesis, the *Clytia* planula normally elongates along the oral-aboral axis and
456 becomes oval in shape (Fig. 4A). By contrast, after *CheWnt3* morpholino injection, the
457 morphant loses oral-aboral axis polarity and exhibits a spherical shape[10]. This raises the
458 possibility that knockdown of *CheWnt3* via siRNA may result in a similar spherical
459 morphology for *Clytia* larvae as is observed in *CheWnt3* morphants. Therefore, to
460 evaluate siRNA knockdown effects on *Clytia*, we chose *CheWnt3* as our second target.
461 We used a mixture of two different siRNAs (1:1 ratio) targeting *CheWnt3*, and
462 carried out electroporation of the siRNA mix into *Clytia* fertilized eggs. After
463 electroporation of *CheWnt3* siRNAs, 1 dpf planula larvae showed nearly complete
464 spherical morphology (Fig. 4B), which is reminiscent of *CheWnt3* morphants[10]. To

465 quantify the effect of siRNA knockdown on *Clytia* larval morphology, we calculated the
466 aspect ratio in two dimensions, where values greater than 1.0 shows the tendency to be
467 oval (ellipsoid-like) while a value of 1.0 indicates a perfect circle (sphere) (Fig. 4C). The
468 control larvae with 0 ng/μl siRNA showed a median aspect ratio of 1.69, indicating a
469 typical ellipsoid-like morphology. By contrast, larvae that underwent electroporation with
470 *CheWnt3* siRNAs (400 ng/μl) showed a median aspect ratio of 1.16, suggesting a much
471 greater tendency toward spherical morphology (Fig. 4D). These results quantitively
472 confirmed the effect of *CheWnt*3 knockdown on larval morphology, which phenocopies
473 *CheWnt3* morphants[10]. To analyze the level of gene-specific knockdown at varying
474 doses of siRNAs, we next electroporated mixtures of 0, 100, 200, and 400 ng/μl of
475 *CheWnt3* siRNAs into *Clytia* fertilized eggs (Figs. 4E-4H). To evaluate *CheWnt3* siRNA
476 effects on morphology, we classified 1 dpf planulae with elongated ellipsoid-like shapes
477 as "normal" and planulae with spherical shapes as "spherical" (Figs. 4I and 4J). The
478 percentage of normal phenotype dramatically reduced after *CheWnt3* siRNA-
479 electroporation (< 1.0 % in 400 ng/μl), even at the lowest dose (5.2% in 100 ng/μl) (Fig.
480 4K). To further evaluate the result at a molecular level, we analyzed relative *CheWnt3*
481 mRNA levels by RT-qPCR and confirmed a significant reduction in *CheWnt3* gene
482 expression at all concentrations (Fig. 4L). Of note, after electroporation with universal
483 negative control siRNA（Nippon Gene Co., Ltd.）, both morphological phenotypes and
484 relative gene expression were comparable to no-siRNA controls (Figs. 4K and 4L),
485 further confirming that siRNA-mediated knockdown by electroporation is target-specific.
486 These results together indicate that siRNAs targeting endogenous genes effectively
487 knock down their expression in *Clytia* embryos.
488 Effective gene knockdown via shRNA electroporation has previously been
489 reported using two cnidarian polyps, *Nematostella vectensis* and *Hydractinia*
490 *symbiolongicarpus*[36,38]. To test whether shRNAs are also effective in the hydrozoan
491 jellyfish *Clytia*, we designed shRNAs targeting *CheWnt3* using the same 19 bp target
492 sequence that was used for siRNAs, and performed electroporation on fertilized eggs
493 with a mix of two different *Wnt3* shRNAs. After electroporation of *Wnt3* shRNAs, relative
494 *Wnt3* mRNA expression in 1 dpf planula was weakly down-regulated (0.83), and was
495 not significant compared to the striking effects of *Wnt3* siRNA electroporation (0.039) at
496 the same concentration (400 ng/μl) (Fig. 4L). In addition, electroporation of *Wnt3*

497 siRNAs resulted in an extensive morphological change toward spherical shaped
498 planulae, showing almost no "normal" phenotype (0.71%), whereas electroporation of
499 shRNA had a limited effect (60.4%) (Fig. 4K). These results suggest that the effect of
500 siRNA is much stronger than that of shRNA in *Clytia* when treated with the same target
501 sequence and concentration.
502
503 **Identification of *Wnt3* in *Cladonema pacificum***
504 In contrast to *Clytia*, the sole genetic model jellyfish, previous studies have neither
505 established genetic manipulation nor performed genome sequencing of *Cladonema*
506 *pacificum*, despite its unique biological features. This is partly because the extremely
507 small size of the *Cladonema* egg makes microinjection difficult. By testing whether
508 siRNA-mediated knockdown via electroporation can work in *Cladonema*, we can start to
509 manipulate genes in *Cladonema* while also demonstrating that siRNA electroporation
510 can be applicable to other jellyfish species. While green fluorescent protein (GFP) is
511 often an easy early target for gene manipulation in emerging organisms, *Cladonema*
512 does not exhibit apparent endogenous green fluorescence expression at any stage,
513 unlike *Clytia*. We instead turned our focus to *Wnt3* as the target for gene knockdown in
514 *Cladonema* since Wnt3 plays an important role in early embryonic development in
515 several cnidarian species[55,56].
516 To identify the *Wnt3* ortholog in *Cladonema*, we utilized RNA-seq results from the
517 *Cladonema* polyp, stolon, and medusa manubrium (data not shown). We performed
518 *Cladonema Wnt3* CDS annotation using the *Clytia* CDS database (MARIMBA, Marine
519 models database: http://marimba.obs-vlfr.fr) and found one contig annotated with *Wnt3*
520 (*CpWnt3*) and multiple *Wnt* genes (Supplementary Figs. 5 and 6). We then performed
521 phylogenic analysis using the neighbor-joining method, and confirmed *CpWnt3*
522 (LC720435) is grouped with medusozoan *Hydra vulgaris* (*HvWnt3*) and *Clytia Wnt3*
523 (*CheWnt3*) rather than Anthozoa *Nematostella* and *Acropora digitifera* (Supplementary
524 Fig. 5A). Multiple sequence alignment further showed highly conserved amino acids
525 sequences among different species including bilaterians and cnidarians (Supplementary
526 Fig. 5B). These findings raise the possibility that *CpWnt3* has a similar function in
527 controlling the Wnt/β-catenin pathway in *Cladonema.*
528

529

530 ***Wnt3* knockdown with siRNA in *Cladonema pacificum***

531 Does *Wnt3* function during *Cladonema* embryogenesis, particularly during axial
532 patterning? Interestingly, *Cladonema* planula larvae do not show a clear elongated
533 shape (Fig. 5A), as observed in *Clytia*. It is thus possible that morphogenesis, including
534 axial patterning and/or Wnt/β-catenin pathway function, differs between these two
535 jellyfish species. It is also possible that the limited elongation in *Cladonema* planulae
536 might hamper phenotypical appearance upon inhibition of Wnt/β-catenin signaling.

537 In order to verify that siRNA electroporation works in *Cladonema* and that *Wnt3*
538 affects axial patterning, we performed electroporation of siRNAs targeting *CpWnt3*. We
539 prepared fertilized *Cladonema* eggs as we did in *Clytia*, and used a mixture of two
540 different siRNAs against *CpWnt3* CDS with a 1:1 ratio (300 ng/μl) and performed
541 electroporation with the previously established parameters (50V, 1 pulse, 25 ms) in
542 fertilized *Cladonema* eggs. After electroporation of siRNAs for *CpWnt3*, planula larvae
543 did not exhibit morphological differences compared to controls（Figs. 5A-5C; median
544 aspect ratio: 1.21 for 0 ng/μl control, 1.16 for 300 ng/μl for si*CpWnt3*）. We then
545 quantified the morphological phenotypes by calculating the aspect ratio of 1 dpf
546 planulae and confirmed that *CpWnt3* knockdown does not cause a significant
547 morphological change (Figs. 5D and 5E), which is consistent with the possibility that
548 *Cladonema* planulae simply exhibit limited elongation.

549 Another possibility that would explain the above result is a defect in the siRNA
550 knockdown itself. To test this potential explanation, we carried out RT-qPCR using
551 mRNA samples from 1 dpf planula after electroporating different concentrations of
552 *CpWnt3* siRNA mix (0, 150, and 300 ng/μl) into fertilized eggs. We confirmed a
553 reduction of *Wnt3* gene expression in an siRNA dose-dependent manner (Fig. 5F),
554 eliminating siRNA knockdown defects as the cause of our initial result.

555 To further confirm whether the Wnt/β-catenin pathway is affected by *Wnt3*
556 knockdown, we examined the gene expression of axial markers *Brachyury* (*CpBra*) and
557 *FoxQ2a* (*CpFoxQ2a*), whose expression are influenced by the Wnt/β-catenin pathway in
558 *Clytia*[10]. From RT-qPCR, we found that *CpWnt3* knockdown causes a decrease in
559 *CpBra* gene expression and an increase in *CpFoxQ2a* gene expression (Supplementary
560 Fig. 7). We also examined *CpBra* expression by *in situ* hybridization and confirmed the

561 reduction of *CpBra* expression on the oral side of planula larvae (Figs. 5G-5I), which is
562 similar to the phenotype exhibited by *CheWnt3* morphants in *Clytia*[10]. Notably, after
563 *CpWnt3* siRNAs electroporation, the rate of metamorphosis from planula to primary
564 polyp decreased dramatically (Supplementary Table 5), implying potential
565 developmental defects upon abrogation of the Wnt/β-catenin pathway. These results
566 suggest that, although overall oral-aboral polarity is less prominent in *Cladonema*
567 compared to *Clytia* at the morphological level, the axial patterning mechanism mediated
568 by Wnt/β-catenin signaling may be conserved between these two jellyfish species.
569
570

571 **Discussion**

572 In this study, we have established a method to knock down endogenous genes in two
573 hydrozoan jellyfish, *Clytia hemisphaerica* and *Cladonema pacificum*, via the siRNA
574 electroporation of fertilized eggs. We showed that knockdown of endogenous *GFP1* in
575 *Clytia* causes the loss of GFP fluorescence in the planula stage (Fig. 3), as previously
576 achieved by CRISPR/Cas9-mediated *GFP1* knockout[11]. We also confirmed that
577 knockdown of *Wnt3* in *Clytia* induces spherical morphology of the planula (Fig. 4),
578 mirroring the results of injections of *Wnt3* morpholino antisense oligo[10]. We further
579 succeeded in efficient repression of *Wnt3* gene expression in *Cladonema* after *Wnt3*
580 siRNA electroporation and found that expression of axial patterning genes is controlled
581 by the Wnt/β-catenin pathway (Fig. 5), suggesting that the conserved mechanism is
582 involved in embryogenesis and planula morphogenesis across hydrozoan jellyfish
583 species.

584 Our results show that the knockdown efficiency of siRNA is much greater than
585 that of shRNA for electroporation of *Clytia* fertilized eggs with the same *Wnt3* target
586 sequence in the same concentration (Fig. 4K-4L). One possibility that would explain
587 such distinct effects between siRNA and shRNA electroporation is the existence of
588 differences in the RNAi machinery or RNA processing efficiency among cnidarians.
589 During RNAi in mammals, the RNase III Dicer protein processes shRNA in collaboration
590 with cofactors TRBP (Transactivation response element RNA-binding protein) and
591 PACT（protein activator of the interferon-induced protein kinase）to produce a mature
592 form of siRNA[39]. Mature siRNA in the Dicer and TRBP/PACT complex is associated

593 with the Argonaute protein and cleaves endogenous complementary mRNAs as the
594 RNA-induced silencing complex [30,57]. These small RNA biogenesis factors, Dicers and
595 cofactors (TRBP in bilaterians, HYL1 in plants and cnidarians), are found in
596 *Nematostella vectensis, Acropora digitifera,* and *Hydra vulgaris*[41]. Although Dicers
597 (TCONS_00004571 and TCONS_00004525) and Hyl1 (TCONS_00010722) are
598 predicted to exist in *Clytia* based on MARIMBA transcriptome data, the expression level
599 of Dicers in oocytes and early gastrulation stages is lower than that in other stages,
600 suggesting the possibility that insufficient shRNA to siRNA processing efficiency is
601 responsible for the difference in knockdown efficiency between siRNA and shRNA
602 electroporation. It will be interesting to elucidate the detailed molecular mechanism of
603 RNAi in different cnidarian species and address RNA processing efficiency in distinct
604 developmental stages. The lower efficiency of knockdown by shRNA compared to
605 siRNA in *Clytia* could also be simply explained by lower shRNA electroporation
606 efficiency. This possibility could be tested by inserting shRNA or siRNA into fertilized
607 eggs by microinjection, instead of electroporation, which would be followed by
608 assessing gene expression and phenotypes.
609 During *Clytia* early embryogenesis, *Wnt3* RNA is localized to the animal cortex of
610 the egg and contributes to the formation of the oral-aboral axis[10]. Accordingly,
611 knockdown of *Wnt3* in *Clytia* fertilized eggs induces suppression of axis formation and
612 planula elongation (Fig. 4). In contrast, despite the fact that no morphological phenotype
613 was observed after *Wnt3* knockdown in *Cladonema*, gene expression of the conserved
614 axial patterning genes, *Brachyury* and *FoxQ2a,* was disrupted (Figs. 5G-5H and
615 Supplementary Fig. 7). In addition to *Clytia,* the Wnt/β-catenin pathway is involved in
616 axis formation during cnidarian embryogenesis including *Nematostella*[44,55,58],
617 *Acropora*[59], *and Hydractinia*[56]. Furthermore, given that the Wnt/β-catenin pathway is
618 also associated with axis formation during metamorphosis in *Hydractinia*[56,60] and
619 *Clytia*[61], the reduced metamorphosis rate observed in *CpWnt3* knockdown *Cladonema*
620 may be attributed to disrupted axis formation (Supplementary Table 5). Taken together,
621 our data support the pivotal role of Wnt/β-catenin signaling in cnidarian development.
622 Why do *Cladonema* planulae show a less elongated morphology during the
623 transition from embryos? In the torpedo-shaped *Clytia* planula, the Wnt/Planar Cell
624 Polarity (PCP) pathway is activated during the gastrulation phase, which causes

625 elongation of the body axis[62]. In contrast, the PCP pathway is independent of the Wnt/β-
626 catenin pathway in *Nematostella*, which have relatively short planula morphology[63]. It is
627 thus possible that the Wnt/PCP pathway is not associated with cell polarity and
628 elongation in *Cladonema*, but more detailed studies are needed.
629 An interesting feature of jellyfish is that their morphology dramatically changes
630 across their life cycle from planula to polyp and then to medusa. In particular, polyps
631 and medusae, different adult stages of the same animal, exhibit distinct regenerative
632 ability, lifespan, and behaviors. Although regeneration mechanisms have been
633 extensively studied in polyp-only animals such as *Hydra* and *Hydractinia*, classical
634 studies have used the medusa stage of several jellyfish species and demonstrated their
635 regenerative potential[21]. Recent work using *Clytia* medusae has further shown a
636 remarkable remodeling and repatterning mechanism orchestrated by muscle systems
637 upon organ loss[17]. At the behavior level, the medusae of the upside-down
638 jellyfish *Cassiopea* exhibit a sleep-like state[64], which is similarly observed in *Hydra*
639 polyps[65]. More recent work using transgenic *Clytia* has characterized feeding behaviors
640 in medusae at a neural-network resolution[19]. To understand how these diverse
641 biological processes in jellyfish are regulated at the molecular level, the functions of
642 specific genes at various stages must be analyzed. Although gene knockdown by
643 dsRNA electroporation into polyps in the scyphozoan jellyfish *Aurelia* has been
644 reported[66], genetic manipulation in medusae has not yet been achieved. Given that
645 siRNA electroporation is applicable to *Hydra* polyps[33,67] in addition to cnidarian fertilized
646 eggs, we now have a better chance to apply this technique to the medusa stage,
647 although, because they are susceptible to electric shock, electroporation parameters
648 must be optimized in order to achieve gene knockdown in medusae. Collectively, our
649 gene knockdown via siRNA electroporation method will complement the existing shRNA
650 electroporation approach in cnidarian polyps and will enable molecular-level analysis of
651 the vast biological phenomena exhibited across the different life stages in jellyfish.
652
653
654 **References**
655 1 Technau, U. & Steele, R. E. Evolutionary crossroads in developmental biology:
656 Cnidaria. *Development* **138**, 1447-1458, doi:10.1242/dev.048959 (2011).

657 2 Zapata, F. *et al.* Phylogenomic Analyses Support Traditional Relationships within
658 Cnidaria. *PLoS One* **10**, e0139068, doi:10.1371/journal.pone.0139068 (2015).
659 3 Leclere, L. & Rottinger, E. Diversity of Cnidarian Muscles: Function, Anatomy,
660 Development and Regeneration. *Front Cell Dev Biol* **4**, 157,
661 doi:10.3389/fcell.2016.00157 (2016).
662 4 Holstein, T. W., Hobmayer, E. & Technau, U. Cnidarians: an evolutionarily
663 conserved model system for regeneration? *Dev Dyn* **226**, 257-267,
664 doi:10.1002/dvdy.10227 (2003).
665 5 Bosch, T. C. G. *et al.* Back to the Basics: Cnidarians Start to Fire. *Trends*
666 *Neurosci* **40**, 92-105, doi:10.1016/j.tins.2016.11.005 (2017).
667 6 Houliston, E., Momose, T. & Manuel, M. Clytia hemisphaerica: a jellyfish cousin
668 joins the laboratory. *Trends Genet* **26**, 159-167, doi:10.1016/j.tig.2010.01.008
669 (2010).
670 7 Houliston, E., Leclere, L., Munro, C., Copley, R. R. & Momose, T. Past, present
671 and future of Clytia hemisphaerica as a laboratory jellyfish. *Curr Top Dev Biol*,
672 doi:10.1016/bs.ctdb.2021.12.014 (2022).
673 8 Lechable, M. *et al.* An improved whole life cycle culture protocol for the
674 hydrozoan genetic model Clytia hemisphaerica. *Biol Open* **9**,
675 doi:10.1242/bio.051268 (2020).
676 9 Momose, T. & Houliston, E. Two oppositely localised frizzled RNAs as axis
677 determinants in a cnidarian embryo. *PLoS Biol* **5**, e70,
678 doi:10.1371/journal.pbio.0050070 (2007).
679 10 Momose, T., Derelle, R. & Houliston, E. A maternally localised Wnt ligand
680 required for axial patterning in the cnidarian Clytia hemisphaerica. *Development*
681 **135**, 2105-2113, doi:10.1242/dev.021543 (2008).
682 11 Momose, T. *et al.* High doses of CRISPR/Cas9 ribonucleoprotein efficiently
683 induce gene knockout with low mosaicism in the hydrozoan Clytia hemisphaerica
684 through microhomology-mediated deletion. *Sci Rep* **8**, 11734,
685 doi:10.1038/s41598-018-30188-0 (2018).
686 12 Quiroga Artigas, G. *et al.* A gonad-expressed opsin mediates light-induced
687 spawning in the jellyfish Clytia. *Elife* **7**, doi:10.7554/eLife.29555 (2018).

688 13 Quiroga Artigas, G. *et al.* A G protein-coupled receptor mediates neuropeptide-
689 induced oocyte maturation in the jellyfish Clytia. *PLoS Biol* **18**, e3000614,
690 doi:10.1371/journal.pbio.3000614 (2020).
691 14 Lapebie, P. *et al.* Differential responses to Wnt and PCP disruption predict
692 expression and developmental function of conserved and novel genes in a
693 cnidarian. *PLoS Genet* **10**, e1004590, doi:10.1371/journal.pgen.1004590 (2014).
694 15 Condamine, T. *et al.* Molecular characterisation of a cellular conveyor belt in
695 Clytia medusae. *Dev Biol* **456**, 212-225, doi:10.1016/j.ydbio.2019.09.001 (2019).
696 16 Leclere, L. *et al.* The genome of the jellyfish Clytia hemisphaerica and the
697 evolution of the cnidarian life-cycle. *Nat Ecol Evol* **3**, 801-810,
698 doi:10.1038/s41559-019-0833-2 (2019).
699 17 Sinigaglia, C. *et al.* Pattern regulation in a regenerating jellyfish. *Elife* **9**,
700 doi:10.7554/eLife.54868 (2020).
701 18 Chari, T. *et al.* Whole-animal multiplexed single-cell RNA-seq reveals
702 transcriptional shifts across Clytia medusa cell types. *Sci Adv* **7**, eabh1683,
703 doi:10.1126/sciadv.abh1683 (2021).
704 19 Weissbourd, B. *et al.* A genetically tractable jellyfish model for systems and
705 evolutionary neuroscience. *Cell* **184**, 5854-5868 e5820,
706 doi:10.1016/j.cell.2021.10.021 (2021).
707 20 Leclere, L. *et al.* Maternally localized germ plasm mRNAs and germ cell/stem cell
708 formation in the cnidarian Clytia. *Dev Biol* **364**, 236-248,
709 doi:10.1016/j.ydbio.2012.01.018 (2012).
710 21 Fujita, S., Kuranaga, E. & Nakajima, Y. I. Regeneration Potential of Jellyfish:
711 Cellular Mechanisms and Molecular Insights. *Genes (Basel)* **12**,
712 doi:10.3390/genes12050758 (2021).
713 22 Fujiki, A., Hou, S., Nakamoto, A. & Kumano, G. Branching pattern and
714 morphogenesis of medusa tentacles in the jellyfish Cladonema pacificum
715 (Hydrozoa, Cnidaria). *Zoological Lett* **5**, 12, doi:10.1186/s40851-019-0124-4
716 (2019).
717 23 Fujita, S., Kuranaga, E. & Nakajima, Y. I. Cell proliferation controls body size
718 growth, tentacle morphogenesis, and regeneration in hydrozoan jellyfish
719 Cladonema pacificum. *PeerJ* **7**, e7579, doi:10.7717/peerj.7579 (2019).

720 24 Hou, S., Zhu, J., Shibata, S., Nakamoto, A. & Kumano, G. Repetitive
721 accumulation of interstitial cells generates the branched structure of Cladonema
722 medusa tentacles. *Development* **148**, doi:10.1242/dev.199544 (2021).
723 25 Takeda, N. *et al.* Identification of jellyfish neuropeptides that act directly as
724 oocyte maturation-inducing hormones. *Development* **145**,
725 doi:10.1242/dev.156786 (2018).
726 26 Stierwald, M., Yanze, N., Bamert, R. P., Kammermeier, L. & Schmid, V. The Sine
727 oculis/Six class family of homeobox genes in jellyfish with and without eyes:
728 development and eye regeneration. *Dev Biol* **274**, 70-81,
729 doi:10.1016/j.ydbio.2004.06.018 (2004).
730 27 Suga, H., Schmid, V. & Gehring, W. J. Evolution and functional diversity of
731 jellyfish opsins. *Curr Biol* **18**, 51-55, doi:10.1016/j.cub.2007.11.059 (2008).
732 28 Suga, H. *et al.* Flexibly deployed Pax genes in eye development at the early
733 evolution of animals demonstrated by studies on a hydrozoan jellyfish. *Proc Natl*
734 *Acad Sci U S A* **107**, 14263-14268, doi:10.1073/pnas.1008389107 (2010).
735 29 Graziussi, D. F., Suga, H., Schmid, V. & Gehring, W. J. The "eyes absent" (eya)
736 gene in the eye-bearing hydrozoan jellyfish Cladonema radiatum: conservation of
737 the retinal determination network. *J Exp Zool B Mol Dev Evol* **318**, 257-267,
738 doi:10.1002/jez.b.22442 (2012).
739 30 Meister, G. & Tuschl, T. Mechanisms of gene silencing by double-stranded RNA.
740 *Nature* **431**, 343-349, doi:10.1038/nature02873 (2004).
741 31 Rao, D. D., Vorhies, J. S., Senzer, N. & Nemunaitis, J. siRNA vs. shRNA:
742 similarities and differences. *Adv Drug Deliv Rev* **61**, 746-759,
743 doi:10.1016/j.addr.2009.04.004 (2009).
744 32 Moran, Y. *et al.* Cnidarian microRNAs frequently regulate targets by cleavage.
745 *Genome Res* **24**, 651-663, doi:10.1101/gr.162503.113 (2014).
746 33 Watanabe, H. *et al.* Nodal signalling determines biradial asymmetry in Hydra.
747 *Nature* **515**, 112-115, doi:10.1038/nature13666 (2014).
748 34 Pankow, S. & Bamberger, C. The p53 tumor suppressor-like protein nvp63
749 mediates selective germ cell death in the sea anemone Nematostella vectensis.
750 *PLoS One* **2**, e782, doi:10.1371/journal.pone.0000782 (2007).

751 35 He, S. *et al.* An axial Hox code controls tissue segmentation and body patterning
752 in Nematostella vectensis. *Science* **361**, 1377-1380,
753 doi:10.1126/science.aar8384 (2018).
754 36 Karabulut, A., He, S., Chen, C. Y., McKinney, S. A. & Gibson, M. C.
755 Electroporation of short hairpin RNAs for rapid and efficient gene knockdown in
756 the starlet sea anemone, Nematostella vectensis. *Dev Biol* **448**, 7-15,
757 doi:10.1016/j.ydbio.2019.01.005 (2019).
758 37 DuBuc, T. Q. *et al.* Transcription factor AP2 controls cnidarian germ cell
759 induction. *Science* **367**, 757-762, doi:10.1126/science.aay6782 (2020).
760 38 Quiroga-Artigas, G., Duscher, A., Lundquist, K., Waletich, J. & Schnitzler, C. E.
761 Gene knockdown via electroporation of short hairpin RNAs in embryos of the
762 marine hydroid Hydractinia symbiolongicarpus. *Sci Rep* **10**, 12806,
763 doi:10.1038/s41598-020-69489-8 (2020).
764 39 Ha, M. & Kim, V. N. Regulation of microRNA biogenesis. *Nat Rev Mol Cell Biol*
765 **15**, 509-524, doi:10.1038/nrm3838 (2014).
766 40 Krishna, S. *et al.* Deep sequencing reveals unique small RNA repertoire that is
767 regulated during head regeneration in Hydra magnipapillata. *Nucleic Acids Res*
768 **41**, 599-616, doi:10.1093/nar/gks1020 (2013).
769 41 Moran, Y., Praher, D., Fredman, D. & Technau, U. The evolution of microRNA
770 pathway protein components in Cnidaria. *Mol Biol Evol* **30**, 2541-2552,
771 doi:10.1093/molbev/mst159 (2013).
772 42 Murchison, E. P., Partridge, J. F., Tam, O. H., Cheloufi, S. & Hannon, G. J.
773 Characterization of Dicer-deficient murine embryonic stem cells. *Proc Natl Acad*
774 *Sci U S A* **102**, 12135-12140, doi:10.1073/pnas.0505479102 (2005).
775 43 Kok, K. H., Ng, M. H., Ching, Y. P. & Jin, D. Y. Human TRBP and PACT directly
776 interact with each other and associate with dicer to facilitate the production of
777 small interfering RNA. *J Biol Chem* **282**, 17649-17657,
778 doi:10.1074/jbc.M611768200 (2007).
779 44 Watanabe, H. *et al.* Sequential actions of beta-catenin and Bmp pattern the oral
780 nerve net in Nematostella vectensis. *Nat Commun* **5**, 5536,
781 doi:10.1038/ncomms6536 (2014).

782 45 Schindelin, J. *et al.* Fiji: an open-source platform for biological-image analysis.
783 *Nat Methods* **9**, 676-682, doi:10.1038/nmeth.2019 (2012).
784 46 Thompson, J. D., Higgins, D. G. & Gibson, T. J. CLUSTAL W: improving the
785 sensitivity of progressive multiple sequence alignment through sequence
786 weighting, position-specific gap penalties and weight matrix choice. *Nucleic Acids*
787 *Res* **22**, 4673-4680, doi:10.1093/nar/22.22.4673 (1994).
788 47 Waterhouse, A. M., Procter, J. B., Martin, D. M., Clamp, M. & Barton, G. J.
789 Jalview Version 2--a multiple sequence alignment editor and analysis workbench.
790 *Bioinformatics* **25**, 1189-1191, doi:10.1093/bioinformatics/btp033 (2009).
791 48 Kumar, S., Stecher, G., Li, M., Knyaz, C. & Tamura, K. MEGA X: Molecular
792 Evolutionary Genetics Analysis across Computing Platforms. *Mol Biol Evol* **35**,
793 1547-1549, doi:10.1093/molbev/msy096 (2018).
794 49 Deguchi, R., Kondoh, E. & Itoh, J. Spatiotemporal characteristics and
795 mechanisms of intracellular Ca(2+) increases at fertilization in eggs of jellyfish
796 (Phylum Cnidaria, Class Hydrozoa). *Dev Biol* **279**, 291-307,
797 doi:10.1016/j.ydbio.2004.11.036 (2005).
798 50 Scholz, C. B. & Technau, U. The ancestral role of Brachyury: expression of
799 NemBra1 in the basal cnidarian Nematostella vectensis (Anthozoa). *Dev Genes*
800 *Evol* **212**, 563-570, doi:10.1007/s00427-002-0272-x (2003).
801 51 Servetnick, M. D. *et al.* Cas9-mediated excision of Nematostella brachyury
802 disrupts endoderm development, pharynx formation and oral-aboral patterning.
803 *Development* **144**, 2951-2960, doi:10.1242/dev.145839 (2017).
804 52 Fourrage, C., Swann, K., Gonzalez Garcia, J. R., Campbell, A. K. & Houliston, E.
805 An endogenous green fluorescent protein-photoprotein pair in Clytia
806 hemisphaerica eggs shows co-targeting to mitochondria and efficient
807 bioluminescence energy transfer. *Open Biol* **4**, 130206, doi:10.1098/rsob.130206
808 (2014).
809 53 Guder, C. *et al.* The Wnt code: cnidarians signal the way. *Oncogene* **25**, 7450-
810 7460, doi:10.1038/sj.onc.1210052 (2006).
811 54 Lee, P. N., Pang, K., Matus, D. Q. & Martindale, M. Q. A WNT of things to come:
812 evolution of Wnt signaling and polarity in cnidarians. *Semin Cell Dev Biol* **17**,
813 157-167, doi:10.1016/j.semcdb.2006.05.002 (2006).

814 55 Kraus, Y., Aman, A., Technau, U. & Genikhovich, G. Pre-bilaterian origin of the
815 blastoporal axial organizer. *Nat Commun* **7**, 11694, doi:10.1038/ncomms11694
816 (2016).
817 56 Plickert, G., Jacoby, V., Frank, U., Muller, W. A. & Mokady, O. Wnt signaling in
818 hydroid development: formation of the primary body axis in embryogenesis and
819 its subsequent patterning. *Dev Biol* **298**, 368-378,
820 doi:10.1016/j.ydbio.2006.06.043 (2006).
821 57 Bartel, D. P. MicroRNAs: genomics, biogenesis, mechanism, and function. *Cell*
822 **116**, 281-297, doi:10.1016/s0092-8674(04)00045-5 (2004).
823 58 DuBuc, T. Q., Stephenson, T. B., Rock, A. Q. & Martindale, M. Q. Hox and Wnt
824 pattern the primary body axis of an anthozoan cnidarian before gastrulation. *Nat*
825 *Commun* **9**, 2007, doi:10.1038/s41467-018-04184-x (2018).
826 59 Yasuoka, Y., Shinzato, C. & Satoh, N. The Mesoderm-Forming Gene brachyury
827 Regulates Ectoderm-Endoderm Demarcation in the Coral Acropora digitifera.
828 *Curr Biol* **26**, 2885-2892, doi:10.1016/j.cub.2016.08.011 (2016).
829 60 Duffy, D. J., Plickert, G., Kuenzel, T., Tilmann, W. & Frank, U. Wnt signaling
830 promotes oral but suppresses aboral structures in Hydractinia metamorphosis
831 and regeneration. *Development* **137**, 3057-3066, doi:10.1242/dev.046631
832 (2010).
833 61 Krasovec, G., Pottin, K., Rosello, M., Queinnec, E. & Chambon, J. P. Apoptosis
834 and cell proliferation during metamorphosis of the planula larva of Clytia
835 hemisphaerica (Hydrozoa, Cnidaria). *Dev Dyn* **250**, 1739-1758,
836 doi:10.1002/dvdy.376 (2021).
837 62 Momose, T., Kraus, Y. & Houliston, E. A conserved function for Strabismus in
838 establishing planar cell polarity in the ciliated ectoderm during cnidarian larval
839 development. *Development* **139**, 4374-4382, doi:10.1242/dev.084251 (2012).
840 63 Kumburegama, S., Wijesena, N., Xu, R. & Wikramanayake, A. H. Strabismus-
841 mediated primary archenteron invagination is uncoupled from Wnt/beta-catenin-
842 dependent endoderm cell fate specification in Nematostella vectensis (Anthozoa,
843 Cnidaria): Implications for the evolution of gastrulation. *Evodevo* **2**, 2,
844 doi:10.1186/2041-9139-2-2 (2011).

845 64 Nath, R. D. *et al.* The Jellyfish Cassiopea Exhibits a Sleep-like State. *Curr Biol*
846 **27**, 2984-2990 e2983, doi:10.1016/j.cub.2017.08.014 (2017).
847 65 Kanaya, H. J. *et al.* A sleep-like state in Hydra unravels conserved sleep
848 mechanisms during the evolutionary development of the central nervous system.
849 *Sci Adv* **6**, doi:10.1126/sciadv.abb9415 (2020).
850 66 Fuchs, B. *et al.* Regulation of polyp-to-jellyfish transition in Aurelia aurita. *Curr*
851 *Biol* **24**, 263-273, doi:10.1016/j.cub.2013.12.003 (2014).
852 67 Lommel, M. *et al.* Hydra Mesoglea Proteome Identifies Thrombospondin as a
853 Conserved Component Active in Head Organizer Restriction. *Sci Rep* **8**, 11753,
854 doi:10.1038/s41598-018-30035-2 (2018).
855
856

857 ## Acknowledgement

858 We thank R. Deguchi (Miyagi Univ. Education, Japan) for sharing *Cladonema pacificum*
859 and EMBRC France for sharing *Clytia hemisphaerica*. We thank T. Momose (Sorbonne
860 University, CNRS, France) for helpful discussion. We thank I. Nagai, H. Nakatani, and
861 A. Sasaki for technical assistance; and A. Dahal, A. Tanimoto, and J. Higuchi for
862 *Nematostella* culture. This work was supported by JST grant number JPMJCR1852 to
863 E.K., AMED under grant number JP21gm6110025 to Y.N., and the JSPS KAKENHI
864 grant numbers JP21H05255 to E.K., and JP17H06332, JP19K22550, JP22H02762 to
865 Y.N.
866
867

868 ## Author contributions

869 T.M.-O. conceptualized and designed the project, performed experiments using jellyfish,
870 analyzed data, prepared figures, and wrote the manuscript. S.F. performed experiments
871 and analyzed data. R.N. performed experiments using *Nematostella*. H.W.
872 conceptualized and designed the project. E.K. contributed reagents. Y.N.
873 conceptualized and designed the project, prepared figures, and wrote the manuscript.
874 All authors approved the final manuscript.
875
876

## Data availability

The datasets used and/or analysed during the current study are available from the corresponding author on reasonable request and nucleotide sequences are available in the GenBank/EMBL/DDBJ under the accession numbers (*CpWnt1*, LC720432; *CpWnt1b*, LC720433; *CpWnt2*, LC720434; *CpWnt3*, LC720435; *CpWnt5*, LC720436; *CpWnt6*, LC720437; *CpWnt8*, LC720438; *CpWntA*, LC720439; *CpBrachyury*, LC720440; *CpFoxQ2a*, LC720441; *F-actin capping protein subunit beta*, LC720442; *CpEF1alpha*, LC720443).

## Competing interests

The authors declare no competing interests.

## Figure legends

**Figure 1. The hydrozoan jellyfish *Clytia hemisphaerica* and *Cladonema pacificum*.** (**A**) Cladogram depicting the phylogenetic position of cnidarian jellyfish. As the sister group of Bilateria, the phylum Cnidaria is divided into two clades, Anthozoa and Medusozoa, which consists of four classes: Hydrozoa, Staurozoa, Scyphozoa, and Cubozoa. Hydrozoa includes polyp type animals without a medusa stage (e.g. *Hydra* and *Hydractinia*) and jellyfish that have both polyp and medusa stages (e.g. *Clytia* and *Cladonema*). (**B** and **C**) Photos of an adult medusa and the eggs of *Clytia hemisphaerica* (**B**) and *Cladonema pacificum* (**C**). Scale bars: 1 mm for medusae; 100 μm for eggs.

**Figure 2. The electroporation procedure for jellyfish eggs.** (**A**) Schematic of spawning under the 24 h light/dark cycle. *Clytia hemisphaerica* are maintained on a 13 h dark/11 h light cycle. After light stimuli, sperm spawning occurs within 60-90 min and egg spawning occurs within 90-120 min. *Cladonema pacificum* are maintained on a 23.5 h light/0.5 h dark cycle. After dark stimuli, sperm and egg spawning occurs within

909 25 min. (**B**) Fertilized eggs are resuspended in 15% Ficoll/artificial sea water to prevent
910 precipitation of eggs during electroporation. (**C**) Electroporation is performed with the
911 Bio-Rad Gene Pulser Xcell electroporation system and a cuvette with a 4 mm gap. (**D**)
912 Visualization of the Rhodamine-Dextran delivery into eggs by electroporation.
913 Rhodamine is shown in red. While little or no fluorescence was observed in eggs
914 without electroporation (No EP), under the condition of a single 50 V pulse for 25 ms,
915 rhodamine signals were detected in both *Clytia and Cladonema* eggs without cell
916 damage. For clarity, egg outlines are indicated with dashed lines for eggs without
917 electroporation. Scale bars: 200 μm.
918
919
920 **Figure 3**. **Phenotypes of *GFP1* knockdown with siRNA in *Clytia* fertilized eggs.** (**A**)
921 Schematic of the siRNA electroporation procedure using fertilized eggs. Fertilized eggs
922 in 15% Ficoll/artificial sea water mixed with siRNA are incubated for 5 min, and
923 electroporation is conducted after transferring into a cuvette. (**B** and **C**) Phenotypes of
924 *Clytia* 2-day planula after *CheGFP1* siRNA knockdown. (**D**) Boxplots showing the GFP
925 fluorescence intensity mean values in 2-day planula after electroporation of 0 and 600
926 ng/μl siRNAs targeting *CheGFP1*. Center lines indicate the medians; x's denote the
927 means; box limits represent the 25th and 75th percentiles; whiskers show the maximum
928 and minimum values. 0 ng/μl, n=24; 600 ng/μl, n=81. ***p<0.001. (**E**-**H**) Phenotypes of
929 3-day planula after siRNA targeting *CheGFP1* electroporation (0, 150, 300, and 600
930 ng/μl si*CheGFP1*). (**I** and **J**) For quantification of green fluorescence, we classified
931 phenotypes into two categories: planula with ring-like green fluorescence as "wild-type,"
932 and planula with reduced green fluorescence as "reduced". (**K**) Quantification of planula
933 larvae positive for *CheGFP1* (wild-type). Bar plots show the percentage of wild-type
934 phenotype after *CheGFP1* knockdown. Number of examined planula: 0 ng/μl, *n*=82; 150
935 ng/μl, *n*=64; 300 ng/μl, *n*=58; 600 ng/μl, *n*=114. Error bars: maximum and minimum
936 values. Experiments were repeated three times. p-values: 150 ng/μl, p=0.064505; 300
937 ng/μl, p=0.001437; 600 ng/μl, p=0.00066. **p<0.01, ***p<0.001. (**L**) Quantification of
938 *CheGFP1* mRNA expression levels in 3-day planula by RT-qPCR. *CheEF1alpha* was
939 used as an internal control. Bar heights represent mean values of at least three
940 independent experiments. *CheGFP1* expression levels are standardized relative to the

941 control (0 ng/μl) condition. Error bars: standard deviation. Experiments were performed
942 in triplicated and repeated at least three times. p-values: 150 ng/μl, p=0.829361; 300
943 ng/μl, p=0.08588; 600 ng/μl, p=0.037359. *p<0.05. Scale bars: 200 μm.
944
945
946 **Figure 4. Phenotypes of *Wnt3* knockdown with siRNA in *Clytia* fertilized eggs.** (**A**
947 and **B**) Typical phenotypes of *Clytia* 1-day planula. While morphologies of control
948 planula (0 ng/μl) have an elongated oval-shape (A), those of *CheWnt3* siRNA (400
949 ng/μl) are spherical in shape (**B**). (**C**) Schematic of ellipse approximation for planula
950 morphology and calculation of the aspect ratio. The aspect ratio was calculated by
951 dividing the long axis (a) by short axis (b). (**D**) Boxplots showing the aspect ratio of the
952 1-day planula. Center lines show the medians; x's denote the mean values; box limits
953 indicate the 25th and 75th percentiles; whiskers show maximum and minimum values;
954 inner points and outliers are represented by circles. Number of examined planula: 0
955 ng/μl, *n*=127; 400 ng/μl. *n*=25, ***p<0.001. (**E**-**H**) Phenotypes of 1-day planula after
956 siRNA targeting *CheWnt3* electroporation (0, 100, 200, and 400 ng/μl si*CheWnt3*). (**I**
957 and **J**) For morphology quantification, we classified planula phenotypes into two
958 categories: elongated oval shape as "normal" and spherical (circle) shape as
959 "spherical". (**K**) Bar plots show the percentage of normal phenotypes across four
960 different siRNA doses as well as planulae treated with shRNA and siNC, a siRNA
961 universal negative control. Percentages are the mean value and error bars indicate
962 standard deviation. Numbers of examined planula: 0 ng/μl, *n*=127; 100 ng/μl, *n*=75; 200
963 ng/μl, *n*=86; 400 ng/μl, *n*=95. shRNA 400 ng/μl, *n*=288; siNC 400 ng/μl, *n*=45.
964 Experiments were repeated three times. Error bars: maximum and minimum values. p-
965 values: 100 ng/μl, p=0.000599; 200 ng/μl, p=0.000438; 400 ng/μl, p=0.000402; 400
966 ng/μl of shRNA, p=0.031928; 400 ng/μl of siNC, p=0.283359. *p<0.05, ***p<0.001. (**L**)
967 Quantification of *CheWnt3* mRNA levels of 1-day planula by RT-qPCR. *CheEF1alpha*
968 was used as an internal control. Bar heights represent the mean value. *CheWnt3*
969 expression levels are standardized relative to the control (0 ng/μl). Error bars: standard
970 deviation. p-values: 100 ng/μl, p= 0.00799; 200 ng/μl, p= 0.000754; 400 ng/μl, p=
971 0.000733; 400 ng/μl of shRNA, p= 0.095403; 400 ng/μl of siNC, p= 0.900264. **p<0.01,

972 ***p<0.001. n.s., not significant. Experiments were performed in triplicate and repeated
973 at least three times. Scale bars: (A, B, E-H) 400 μm, (I, J) 100 μm.
974
975
976 **Figure 5. Phenotypes of *Wnt3* knockdown with siRNA in *Cladonema* fertilized**
977 **eggs.** (**A**) Typical morphology of *Cladonema* egg and planula. The wild-type
978 *Cladonema* planula larvae exhibit a slight oval shape. To deliver siRNAs targeting
979 *CpWnt3,* electroporation was performed in fertilized eggs (1-cell stage), and phenotypes
980 were confirmed at planula in one day. (**B** and **C**) Phenotypes of 1-day planula after
981 *CpWnt3* siRNA knockdown. (**D**) Schematic of ellipse approximation for planula
982 morphology and calculation of the aspect ratio. The aspect ratio was calculated by
983 dividing the long axis (a) by short axis (b). (**E**) Boxplots showing the aspect ratio of the
984 1-day planula after si*CpWnt3* electroporation (0 and 300 ng/μl). Center lines show the
985 medians; x's denote the mean values; box limits indicate the 25th and 75th percentiles;
986 whiskers show maximum and minimum values; inner points and outliers are
987 represented by circles. Number of examined planulae: 0 ng/μl, *n*=22; 300 ng/μl, *n*=50.
988 p= 0.658303. n.s., not significant. (**F**) Quantification of *CpWnt3* mRNA levels in 1-day
989 planula by RT-qPCR. *CpEF1alpha* was used as an internal control. Bar heights
990 represent the mean value. Error bars indicate standard deviation. *CpWnt3* expression
991 levels are standardized relative to the control (0 ng/μl). Experiments were performed in
992 triplicate and repeated three times. p-values: 150 ng/μl, p= 0.376498; 300 ng/μl, p=
993 0.073956. (**G, H**) Representative *in situ* hybridization (ISH) image of oral *CpBra*
994 expression in 1-day planula for control (G: 0 ng/μl si*CpWnt3*) and *CpWnt3* siRNA (H:
995 300 ng/μl si*CpWnt3*). (**I**) Quantification of *CpBra* expression phenotypes based on ISH
996 images. Stacked bar plots show the percentage of 1-day planulae in each phenotypic
997 class. *CpBra* expression patterns are categorized into three phenotypes (strong, weak
998 and none). 0 ng/μl, *n*=74; 300 ng/μl, *n*=58. Scale bars: (B, C) 200 μm, (G, H) 50 μm.

# Figure 1

Masuda-Ozawa et al.

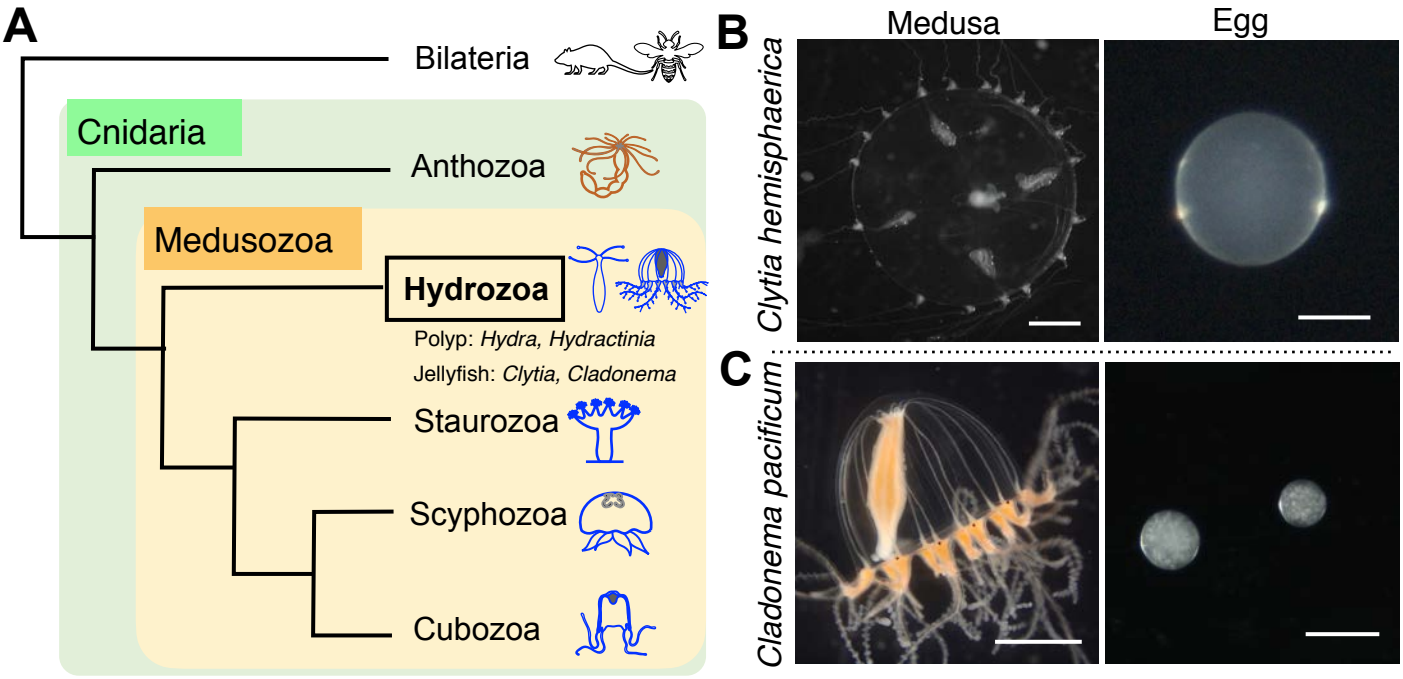

# Figure 2

Masuda-Ozawa et al.

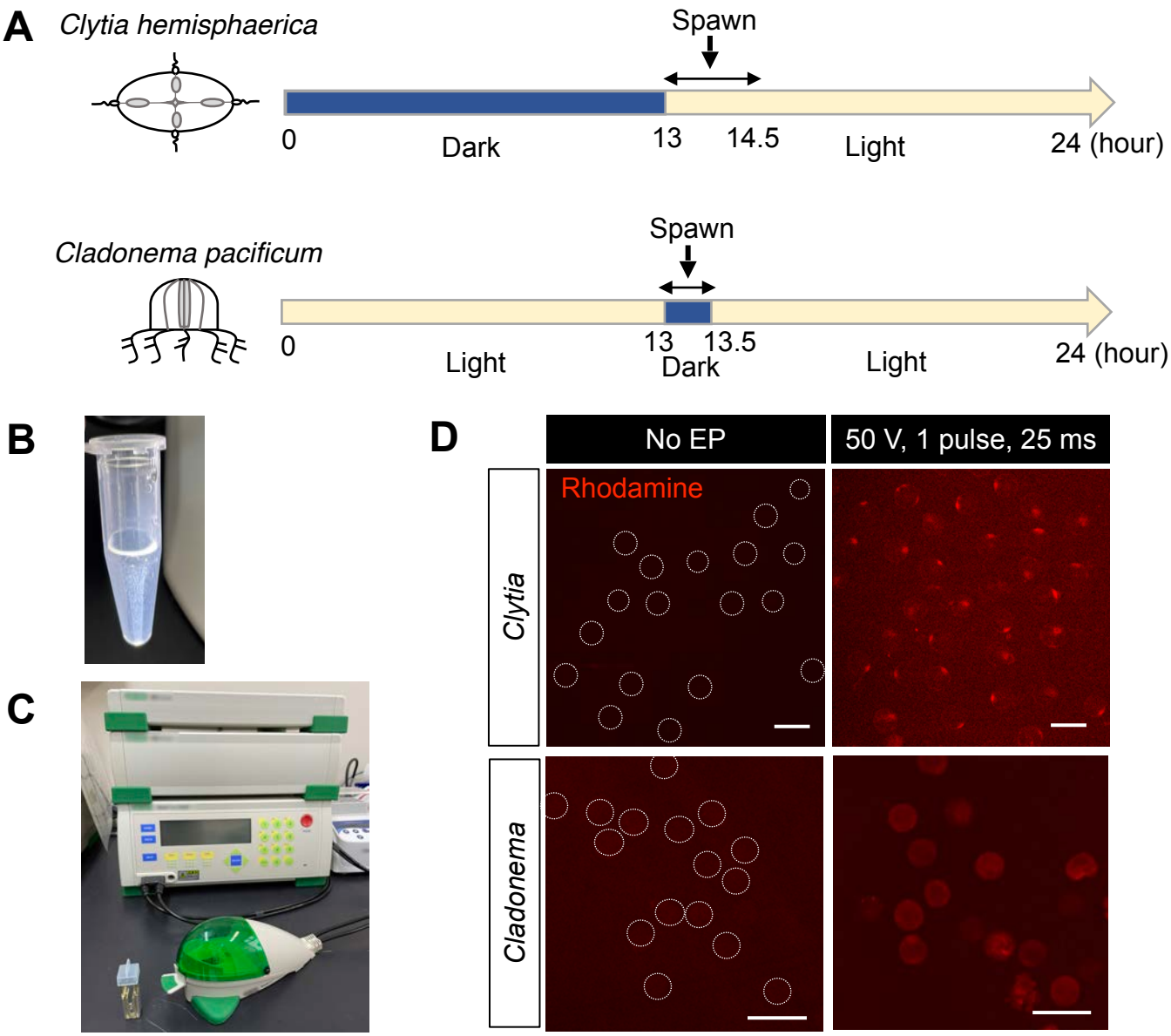

# Figure 3

Masuda-Ozawa et al.

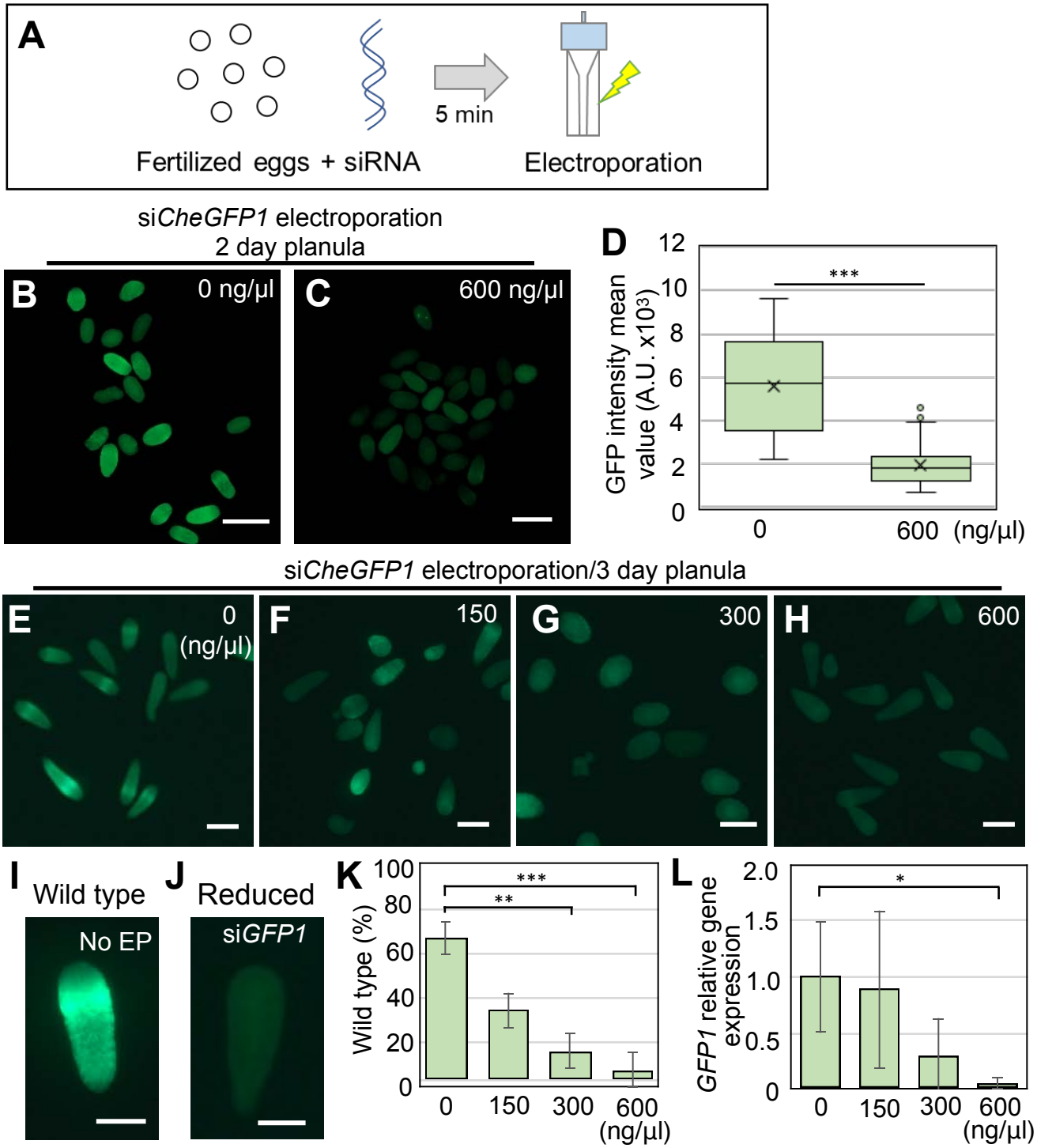

# Figure 4

Masuda-Ozawa et al.

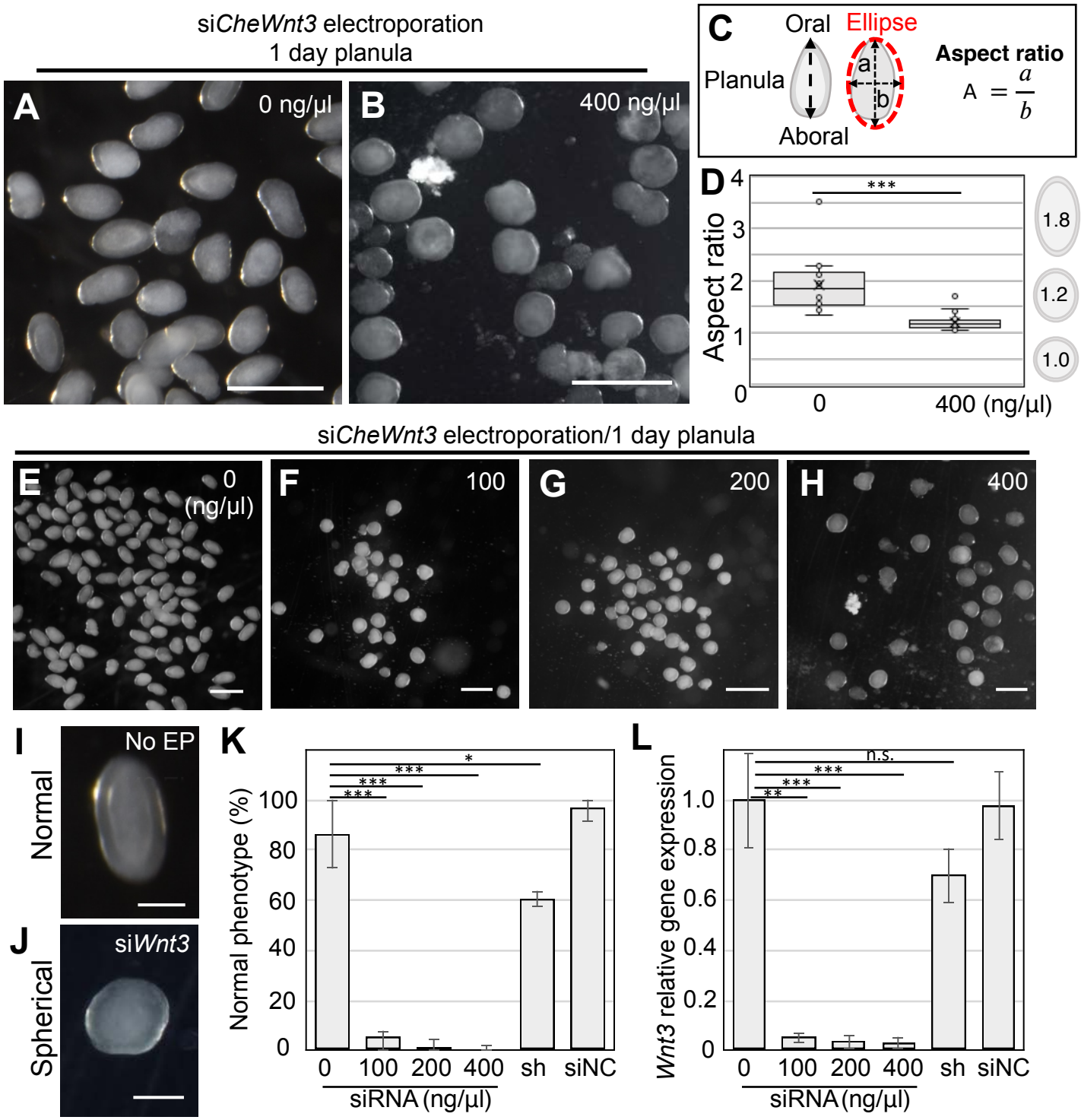

# Figure 5
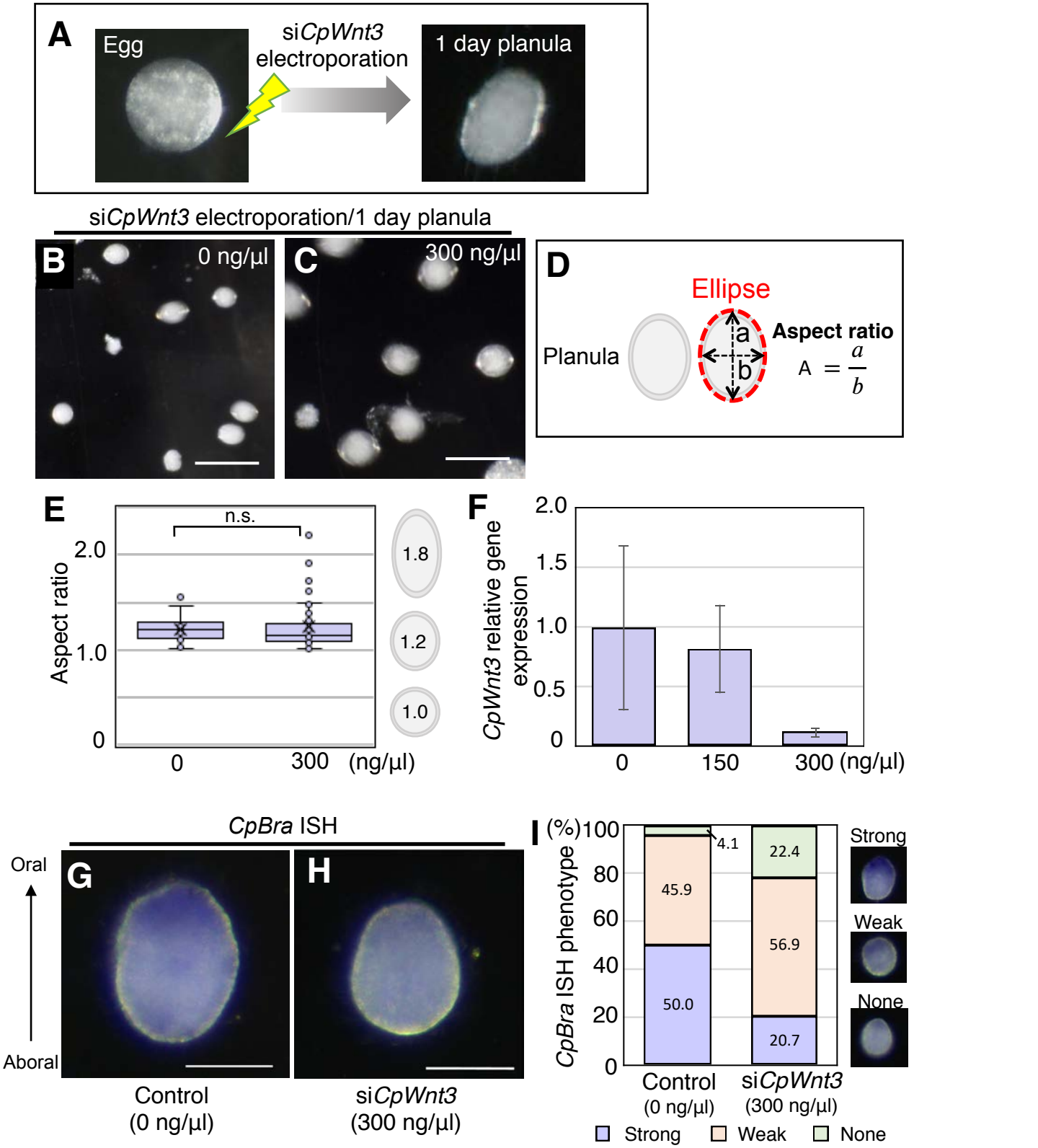
Masuda-Ozawa et al.